Modelling of Smart Transformers for Power System Transient Stability Analysis

Junru Chen, *Member, IEEE*, Muyang Liu, *Member, IEEE*, Terence O'Donnell, *Senior Member, IEEE*, Federico Milano, *Fellow, IEEE*

***Abstract*— The Smart Transformer (ST) has been proposed to enable bidirectional power flows among the several subsystems that compose the smart grid. For an accurate and efficient analysis of the power system dynamic response, a proper ST model must be developed. Starting from the detailed ST model, this paper proposes reduced-order models according to the time scale of the ST dynamics and the simulation objective. The proposed models are classified based on the level of complexity and dynamic order and are compared by means of relevant scenarios, namely, fault (rotor angle stability analysis), DC power exchange (power management) and system contingencies (voltage and frequency stability analysis). Finally, case studies based on the IEEE 39-bus system discuss the features and adequateness of the proposed models in a scenario of an interconnected grid with multiple STs.**

***Index Terms*— Smart Transformer (ST), modeling, power system simulation.**

I. Introduction

A. Motivation

Power systems are migrating to converter-interfaced generation, mostly based on renewable energy resources [1]. An advantage of converter-based generation and control is the ability to develop "smart" solutions that, if properly implemented, can lead to increase the flexibility of the grid. In this context, customers can become "prosumers," i.e., they not only consume but also actively control and produce energy transactions. On the down side, electronic converters introduce more complexity and lead to a mixture of AC and DC subsystems where power flows now are not simply from the feeder to the consumer but are bidirectional among these subsystems. In this new scenario, transformers must be able to manage these bidirectional power flows and, thus, the traditional Low-Frequency Transformer (LFT) is no longer adequate [2]. The ST based on controllable power-electronics converters [3] appears as an ideal energy router [4]. This device can in fact integrate communication networks and smart controllers to provide several services, i.e., power management [5], [6], demand control [7], [8], load identification [9], [10], neutral current control [11], [12] and reactive power compensation [13] as shown in Fig. 1.

Time-domain simulation is a general method for the Transient Stability Assessment (TSA) of the Transmission System Operation (TSO). The configuration of the ST, in general, is 3-stage consisting of MVAC-MVDC, MVDC-LVDC and LVDC-LVAC converters [2]. Because of this complex nature of the ST system, capturing the response of the ST precisely for power system simulations is a challenge. In particular, an over-detailed ST model would increase the computational burden of power system simulations and would typically be unfeasible for large system simulations. To speed up the simulation without loosing accuracy, adequate simplified models are needed. Since approximated models inevitably neglect some dynamic aspect of the ST, this paper focuses on the definition and classification of ST dynamic models based on different levels. A systematic taxonomy is lacking in the literature. This paper fills this gap by proposing simplified ST models and classifies then into 3×3 levels according to their conditions of usage.

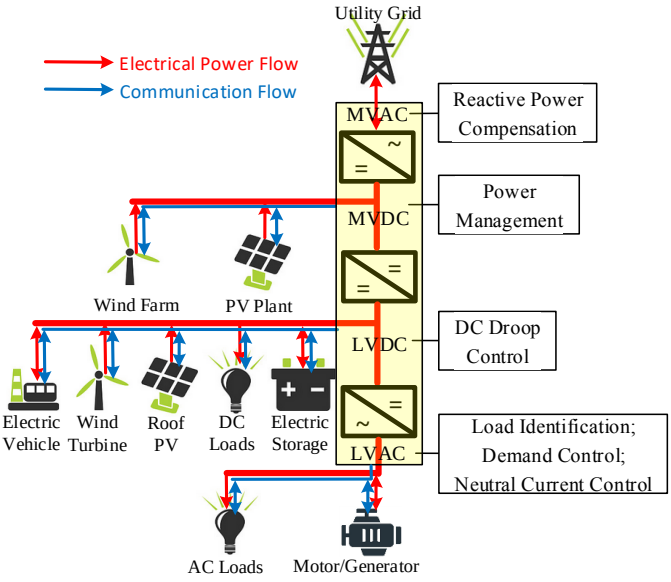

Fig. 1: ST in the power system.

B. Literature Review

The classification for modelling the general power electronics has been proposed in [14] from a simplest phasor model for the optimal power flow use to the complex switching model for the harmonics study. In the power system time-domain dynamic simulation, since the TSO ask a fast computation on the TSA, it is impossible to use switching model for the converters either to model each online generators in detail. As mentioned in [14], for the transient rotor angle stability, voltage and frequency stability, an adequate simplification on the power electronics modelling can speed up the simulation meanwhile remaining a certain level of the accuracy. In

The authors are with the School of Electrical and Electronic Engineering, University College Dublin, Ireland. E-mails: muyang.liu@ucd.ie, junru.chen.1@ucdconnect.ie, and federico.milano@ucd.ie).

This work is supported by the European Commission, by funding Junru Chen and Federico Milano under the Project EdgeFLEX, Grant No. 883710; and by the Science Foundation Ireland, by funding Muyang Liu and Federico Milano, under Investigator Program Grant No. SFI/15/IA/3074.

general, the generators in one power plant are aggregated into a single generator and the electrical equipment are modelled in the form of the Differential-Algebraic Equation (DAE). Even for the DAE model of the Synchronous Generator (SG), it has been classified into several complexities from a classical 2nd order to 8th order, emphasizing from the only electrical transients to a detailed magnetic sub-transient [15].

Specifically for the ST, several models have been proposed in the literature. Reference [16] and [17] proposes a static ST model focusing on the power exchanges among the utility grid and ST-fed internal subsystems. However, this model is developed for economic dispatch studies and power system reliability analysis, thus neglecting all the transients. References [18]–[21] propose a full-order DAE model of a typical three-stage ST with inclusion of detailed control dynamics. These models focus on the power delivery from the primary to the secondary side of the ST. References [22] and [23] extend the full-order DAE model above in order to take into account the DC power integration and the bidirectional power flow. This model can capture the DC voltage dynamics due to the power exchange at the DC ports. However, this model is too detailed to use in a large power system simulation, especially with a very high ST penetrations.

C. Contributions

As discussed above, the existing ST models are either too detailed to satisfy the TSA computational requirement or too simple to capture the dynamics. Intermediate models between the full-order and the purely static can achieve a certain accuracy and meanwhile lower the computational burden. For this purpose, this paper proposes a set of ST DAE models with various levels of approximations for the three stages that compose the ST.

Similarly to the variety of dynamic models that exist for the synchronous machines, the usage of the model depends on the timescale of the interested response and the researching focus. In particular, the larger the time scale, the simpler model of the ST. On the other hand, the interested stages require a precise model while other stages may be simplified. Based on these, the model of the ST can be simplified and classified in different complexities for the different usage conditions. The specific contributions of this paper are:

- To propose and classify simplified ST DAE models according to different simulation time scales and applications and research objectives.
- To benchmarks the proposed simplified ST DAE models against the full DAE model for standard power system transient stability analyses.

D. Organization

The remainder of the paper is organized as follows. Section II introduces the full-order DAE model of the ST. Section III presents the proposed simplified ST models and classifies according to their complexity, time scales and parameter sensitivity analysis. Section IV defines the applications for the the proposed ST models. Section V verifies the accuracy of the proposed models based on the IEEE benchmark 39-bus system. Finally, Section VI draws relevant conclusions.

II. Modeling of the Smart Transformer

Figure 2 shows the configuration of a 3-stage ST, consisting of an MVAC-MVDC Primary Side Converter (PSC) linking to the utility grid; an MVDC-LVDC Dual-Active-Bridge (DAB) with a high frequency transformer; and an LVDC-LVAC Secondary Side Converter (SSC) feeding the distribution system. This provides a link to integrate different kinds of load and generations. In its basic configuration, each stage regulates its port voltage. Additionally the ST can provide primary frequency and voltage support to the system.

For each stage, the model consists of the electric circuit, the basic control functions (e.g. current and voltage) and upper controls for system services. The link between each stage is represented via the dynamics of the power conversion and the voltage control achieved by the upstream converter. The remainder of this section describes the detailed ST model. The notations are explained in Table I and marked in Fig.2.

TABLE I: ST notations.

Notation	Description
ω_g/ω^*	Grid/reference frequency
$\omega_{pll}/\omega_{f,pll}$	PLL/filtered frequency
S_n	ST capability
V_g	Grid voltage
V_{psc}/V_{ssc}	MVAC/LVAC voltage
V_{dcm}/V_{dcl}	MVDC/LVDC voltage
V^*_{psc}/V^*_{ssc}	MVAC/LVAC voltage ref
V^*_{dcm}/V^*_{dcl}	MVDC/LVDC voltage ref
I_{psc}/I_{ssc}	PSC/SSC output current
I^*_{psc}/I^*_{ssc}	PSC/SSC current ref
I_{mvdc}/I_{lvdc}	MVDC/LVDC current to ST
P_{psc}/P_{ssc}	Converted power in PSC/SSC
P_{dab}	Converted power in DAB
P^*_{psc}/Q^*_{psc}	PSC power reference
$m_{psc}/m_{dab}/m_{ssc}$	PSC/DAB/SSC modulation
L_{psc}/r_{psc} and $L_{ssc}/r_{ssc}/C_{ssc}$	PSC and SSC filter
C_{dcm}/C_{dcl}	Capacitor at MVDC/LVDC
n	DAB Transformer ratio
f_m	DAB Transformer frequency
L_m	DAB Transformer inductance
$K_{p,pll}/K_{i,pll}$	PLL parameter P/I
$K_{p,dc}/K_{i,dc}$	DAB voltage controller P/I
$K_{pv,psc}/K_{iv,psc}$	SSC voltage controller P/I
$K_{pc,psc}/K_{ic,psc}$	PSC current controller P/I
$K_{pc,ssc}/K_{ic,ssc}$	SSC current controller P/I
K_v and K_d/K_m	Voltage and frequency support gain
LP_f	Low pass filter gain

A. MVAC-MVDC Primary Side Converter Model

The PSC is an interface of the ST to the MVAC utility grid or transmission system. Its purpose is to feed the total power from the ST-fed subsystems.

The electric circuit in this stage includes the grid power exchange at the Point of Common Coupling (PCC) as shown in Fig. 2 and by the following equations:

$$P_g = V_g \cos(\delta_g - \delta_{pll}) I_{d,psc} + V_g \sin(\delta_g - \delta_{pll}) I_{q,psc}\,,$$
$$Q_g = V_g \sin(\delta_g - \delta_{pll}) I_{d,psc} - V_g \cos(\delta_g - \delta_{pll}) I_{q,psc}\,,$$

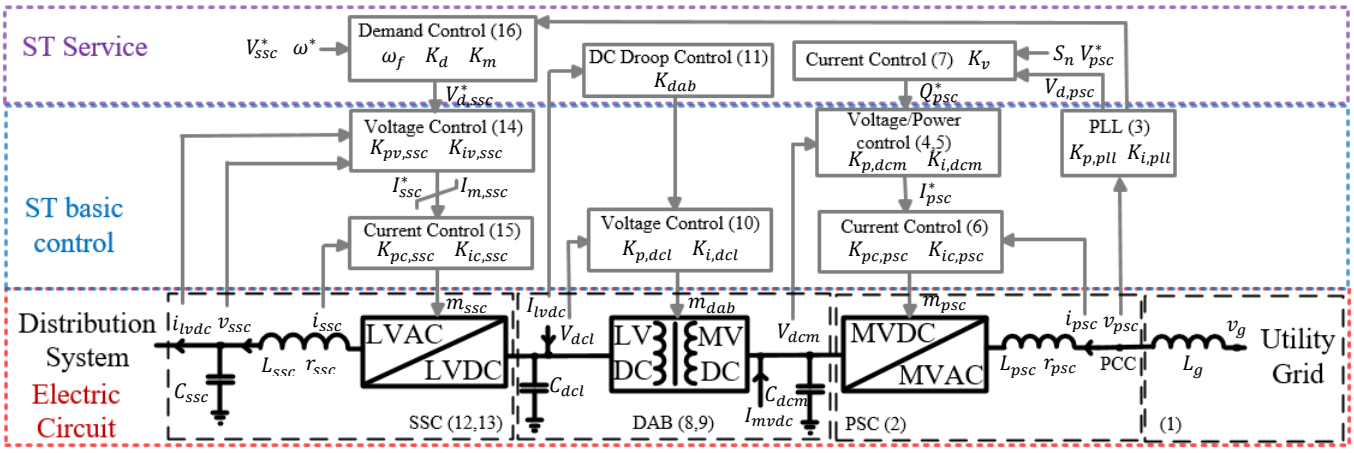

Fig. 2: ST configuration.

$$
\begin{aligned}
V_{d,psc} &= V_g \cos(\delta_g - \delta_{pll}) - \omega_{pll} L_g I_{q,psc} \,, \\
V_{q,psc} &= V_g \sin(\delta_g - \delta_{pll}) + \omega_{pll} L_g I_{d,psc} \,,
\end{aligned} \tag{1}
$$

and the power conversion from the MVAC to the MVDC via the converter modulation and L-filter:

$$
\begin{aligned}
L_{psc}\dot{I}_{d,psc} &= 0.5 m_{d,psc} V_{dcm} - V_{d,psc} \\
&\quad + \omega_{pll} L_{psc} I_{q,psc} - r_{psc} I_{d,psc} \,, \\
L_{psc}\dot{I}_{q,psc} &= 0.5 m_{d,psc} V_{dcm} - V_{q,psc} \\
&\quad - \omega_{pll} L_{psc} I_{d,psc} - r_{psc} I_{q,psc} \,, \\
-C_{dcm} V_{dcm} \dot{V}_{dcm} &= P_{psc} + (V_{d,psc} I_{d,psc} + V_{q,psc} I_{q,psc}) \,.
\end{aligned} \tag{2}
$$

The basic control of the PSC is to maintain the synchronization at the PCC at the MVAC side by means of a Phase-Locked Loop (PLL):

$$
\begin{aligned}
\dot{\delta}_{pll} &= \Delta\omega_{pll} \,, \\
\omega_{pll} &= K_{p,pll} \Delta\omega_{pll} + \mu_{pll} \,, \\
\dot{\mu}_{pll} &= K_{i,pll} \Delta\omega_{pll} \,, \\
\Delta\omega_{pll} &= \omega_g - \omega_{pll} \,,
\end{aligned} \tag{3}
$$

and to regulate the voltage at the MVDC side:

$$
\begin{aligned}
P^*_{psc} &= -K_{p,dcm}(V^{*2}_{dcm} - V^2_{dcm}) + K_{i,dcm}\gamma_{dcm} - P_{psc} \,, \\
\dot{\gamma}_{dcm} &= V^{*2}_{dcm} - V^2_{dcm} \,.
\end{aligned} \tag{4}
$$

The PSC itself uses the outer power inner current control which is defined by:

$$
I^*_{d,psc} = P^*_{psc}/V^*_{psc} \,, \quad \text{and} \quad I^*_{q,psc} = -Q^*_{psc}/V^*_{psc} \,, \tag{5}
$$

to determine the modulation, which links to the electric circuit model, as follows:

$$
\begin{aligned}
0.5 V_{dcm} m_{d,psc} &= K_{pc,psc}(I^*_{d,psc} - I_{d,psc}) \\
&\quad + K_{ic,psc}\epsilon_{d,psc} - \omega_{pll} L_{psc} I_{q,psc} \,, \\
0.5 V_{dcm} m_{q,psc} &= K_{pc,psc}(I^*_{q,psc} - I_{q,psc}) \\
&\quad + K_{ic,psc}\epsilon_{q,psc} + \omega_{pll} L_{psc} I_{d,psc} \,, \\
\dot{\epsilon}_{d,psc} &= I^*_{d,psc} - I_{d,psc} \,, \\
\dot{\epsilon}_{q,psc} &= I^*_{q,psc} - I_{q,psc} \,.
\end{aligned} \tag{6}
$$

The system service provided by the PSC is to support the MVAC voltage at the PCC by means of reactive power compensation:

$$
Q^*_{psc} = \sqrt{\mathrm{S_n}^2 - P^{*2}_{psc}} \left(\frac{V^*_{psc} - V_{d,psc}}{V^*_{psc}}\right) K_v \,. \tag{7}
$$

Note that the principal role of the PSC is to deliver the active power. Thus, the reactive power compensation is limited by the PSC capacity, which determines the power reference of the PSC basic control.

B. MVDC-LVDC Dual-Active Bridge Model

The MVDC-LVDC converter or DAB reduces the voltage level and integrates the DC sources and loads. The electric circuit in this stage includes the power exchange at the MVDC side amongst the PSC, DAB and the MVDC sources and loads:

$$
P_{psc} = I_{mvdc} V_{dcm} + P_{dab} \,, \tag{8}
$$

and the voltage reduction via a high/medium-frequency transformer:

$$
C_{dcl}\dot{V}_{dcl} = \frac{m_{dab}(1 - m_{dab})\, n\, V_{dcm}}{2 f_m L_m} - \frac{P_{dab}}{V_{dcl}} \,. \tag{9}
$$

The basic control of the DAB is to regulate the voltage at the LVDC side:

$$
\begin{aligned}
m_{dab} &= K_{p,dcl}(V^*_{dcl} - V_{dcl}) + K_{i,dcl}\gamma_{dcl} \,, \\
\dot{\gamma}_{dcl} &= V^*_{dcl} - V_{dcl} \,.
\end{aligned} \tag{10}
$$

The service of the DAB is to support the LVDC voltage by means of droop control for the purpose of bidirectional power flow among the subsystems at the LVDC side:

$$
V^*_{dcl} = V_{dcl,max} - K_{dab} I_{lvdc} \,. \tag{11}
$$

C. LVDC-LVAC Secondary Side Converter Model

The SSC links to the distribution system. Its purpose is to form the distribution system via an active voltage control. The electric circuit in this stage includes the power exchange at the

LVDC side amongst the DAB, SSC and the LVDC sources and loads:

$$P_{dab} = I_{lvdc} V_{dcl} + P_{ssc}\,, \tag{12}$$

the power conversion from the LVDC to the LVAC via the converter modulation and the LC-filter:

$$\begin{aligned} L_{ssc}\dot{I}_{d,ssc} &= 0.5 V_{dcl} m_{d,ssc} - V_{d,ssc} \\ &\quad + \omega L_{ssc} I_{q,ssc} - r_{ssc} I_{d,ssc}\,, \\ L_{ssc}\dot{I}_{q,ssc} &= 0.5 m_{d,ssc} V_{dcl} - V_{q,ssc} \\ &\quad - \omega L_{ssc} I_{d,ssc} - r_{ssc} I_{q,ssc}\,, \\ C_{ssc}\dot{V}_{d,ssc} &= I_{d,ssc} - I_{d,lvac} + \omega C_{ssc} V_{q,ssc}, \\ C_{ssc}\dot{V}_{q,ssc} &= I_{q,ssc} - I_{q,lvac} - \omega C_{ssc} V_{d,ssc} \end{aligned} \tag{13}$$

and the power exchange at the PCC with the entire prosumers in the distribution system.

The basic control of the SSC is to regulate the LVAC voltage to determine the modulation and thus, linking to the electric circuit model. It utilizes the outer voltage control:

$$\begin{aligned} I^*_{d,psc} &= K_{pv,ssc}(V^*_{d,ssc} - V_{d,ssc}) + K_{iv,ssc}\gamma_{d,ssc} \\ &\quad - \omega C_{ssc} V_{q,ssc}\,, \\ I^*_{q,psc} &= K_{pv,ssc}(V^*_{q,ssc} - V_{q,ssc}) + K_{iv,ssc}\gamma_{q,ssc} \\ &\quad + \omega C_{ssc} V_{d,ssc}\,, \\ I^{*2}_{m,ssc} &\geq I^{*2}_{d,ssc} + I^{*2}_{q,ssc}\,, \\ \dot{\gamma}_{d,ssc} &= V^*_{d,ssc} - V_{d,ssc}\,, \\ \dot{\gamma}_{q,ssc} &= V^*_{q,ssc} - V_{q,ssc}\,. \end{aligned} \tag{14}$$

and the inner current control:

$$\begin{aligned} 0.5 V_{dcl} m_{d,ssc} &= K_{pc,ssc}(I^*_{d,ssc} - I_{d,ssc}) \\ &\quad + K_{ic,ssc}\epsilon_{d,ssc} - \omega L_{ssc} I_{q,ssc}\,, \\ 0.5 V_{dcl} m_{q,ssc} &= K_{pc,ssc}(I^*_{q,ssc} - I_{q,ssc}) \\ &\quad + K_{ic,ssc}\epsilon_{q,ssc} + \omega L_{ssc} I_{d,ssc}\,, \\ \dot{\epsilon}_{d,ssc} &= I^*_{d,ssc} - I_{d,ssc}\,, \\ \dot{\epsilon}_{q,ssc} &= I^*_{q,ssc} - I_{q,ssc}\,. \end{aligned} \tag{15}$$

The SSC supports the frequency of the utility grid by the means of demand control [8]. The load in general is sensitive to the voltage and using this feature, the SSC can indirectly regulate demand, by actively regulating the LVAC voltage according to the grid frequency and its rate of change. This can be implemented as a higher level control which determines the voltage reference for its basic voltage control. A filter and a dead-band on the frequency measurement is considered to avoid problems with measurement noise. This can be described by the following equations:

$$\begin{aligned} \dot{\omega}_{f,pll} &= -LP_f\ \omega_{f,pll} + LP_f\ \omega_f\,, \\ V^*_{d,ssc} &= (\omega_{f,pll} - \omega^*) K_d + \dot{\omega}_{f,pll} K_m + V^*_{ssc}\,. \end{aligned} \tag{16}$$

Equations (1)-(16) represent the complete 19th-order DAE model of the ST.

D. Model Validation via Hardware Experiment

The full-order DAE ST model is validated via a hardware experiment based on the OPAL-RT platform. A down-scaled 220 V AC to 520 V DC to 245 V AC three phase 2-stage back-to-back converter is utilized in this experiment. The parameters of the hardware setup are given in Table II. The corresponding DAE model is built in Matlab/Simulink. The contingencies are: (i) a grid frequency drop from 50 Hz to 49 Hz with 1 Hz/s ramp at 7 s and following recovery at 10.5 s with 0.5 Hz/s ramp; (ii) a grid voltage step reduction from 1 pu to 0.95 pu at 14.5 s and following recovery to 1 pu at 16 s.

TABLE II: ST hardware set-up.

Parameter	Value
PWM rate	1350
S_n	1500 VA
$K_{pc,psc}/K_{ic,psc}$	331/1700
$K_{p,pll}/K_{i,pll}$	0.73/13
L_{ssc}/r_{ssc}	33 mH/0.12 Ω
$K_{pc,ssc}/K_{ic,ssc}$	331/1700
$K_v/K_d/K_m$	53/3.9/24.5
Sampling time	14.5 μs
L_{psc}/r_{psc}	33 mH/0.12 Ω
$K_{p,dc}/K_{i,dc}$	0.02/0.005
C_{dc}	1.4 mF
C_{ssc}	80 μF
$K_{pv,ssc}/K_{iv,ssc}$	0.27/300
Loading	163Ω/ phase

Figure 3 shows that the DAE model captures the power variations at the PCC of the PSC accurately. However, since the converter switching dynamics are neglected, the DAE model cannot reflect the harmonics at the PWM frequency.

For the downstream subsystems, it is more relevant to observe the supply voltages, i.e., DC voltage and LVAC voltage, which are shown in Fig. 4. The DAE model presents the DC voltage transients during the active and reactive power change at the AC sides. This transient cannot be well observed in the hardware results due to the harmonics at PWM frequency. On the other hand, the DAE model accurately captures the voltage variation at the AC side of the SSC. Note that the reactive power compensation of the PSC only has an impact on the DC voltage but not on the AC voltage of SSC.

E. Model Validation via Simulation

Due to limitations in accessing a fully functional 3 stage SST prototype, the hardware validation experiment only used a 2-stage ST. For a further validation, a 3-stage ST EMT model is built in Matlab/Simulink, the parameters for which are given in Table IV. The time step of the simulation is 0.1 us and the switching frequency of the PSC, DAB and SSC are 1650 Hz,10 kHz and 6.3 kHz respectively. The ST experiences an LVAC load change from 33 Ω to 16.5 Ω at 2 s, an MVAC current change from 0 A to -0.06 A at 2.5 s and an LVAC current change from 0 A to 1.5 A at 3 s.

Figure 5 compares the result from the EMT model and the DAE model. The DAE model can represent the EMT model to a certain accuracy as shown by comparing the results of the MVAC power, MVDC voltage and LVDC voltage in regardless of the PWM harmonics.

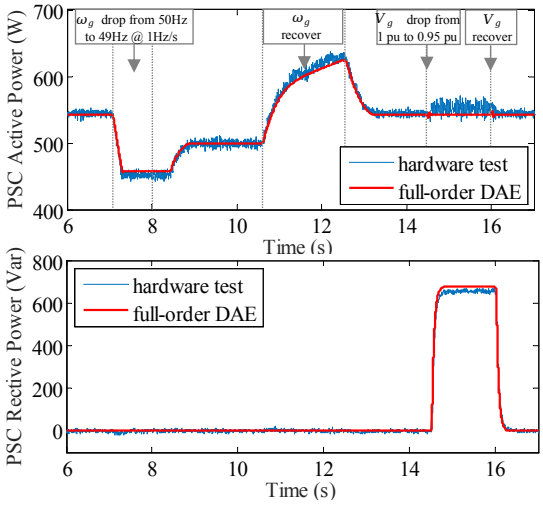

Fig. 3: Validation of the detailed ST model: power exchange with the grid.

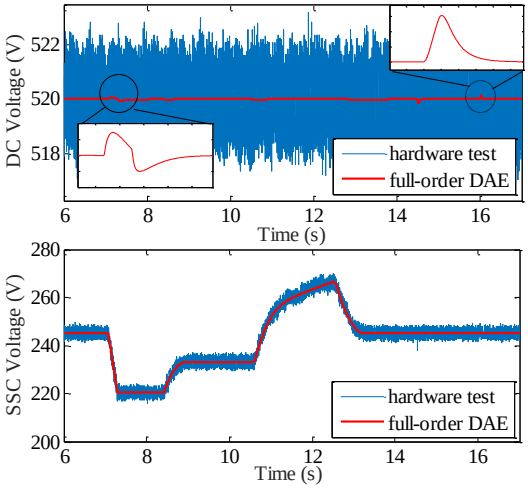

Fig. 4: Validation of the detailed ST model: voltage regulation.

III. Approximated ST Models

Depending on the time constant of the current controllers, the time step to properly integrate the full-order ST has to be in the range of 10 to 100 μs. This leads to a heavy computational burden when considering angle and voltage transient stability studies that typically require simulating several seconds especially in the case of large systems with multiple STs.

The computation burden can be decreased by reducing the dynamic order of the ST model with respect to the system dynamic response (see relevant time scales in Fig. 6). Depending on the focus of study, some of the ST controls can be assumed to be ideal, and thus, its dynamic can be neglected. For example, if one is interested in the system inertial response, the ST current controller transients can be neglected. In the same vein, if the interest is in the system primary response, then only ST higher level controllers and services need to be retained in the model.

Parameter sensitivity is a method which can be used to identify the dependence of the ST model dynamics on the various

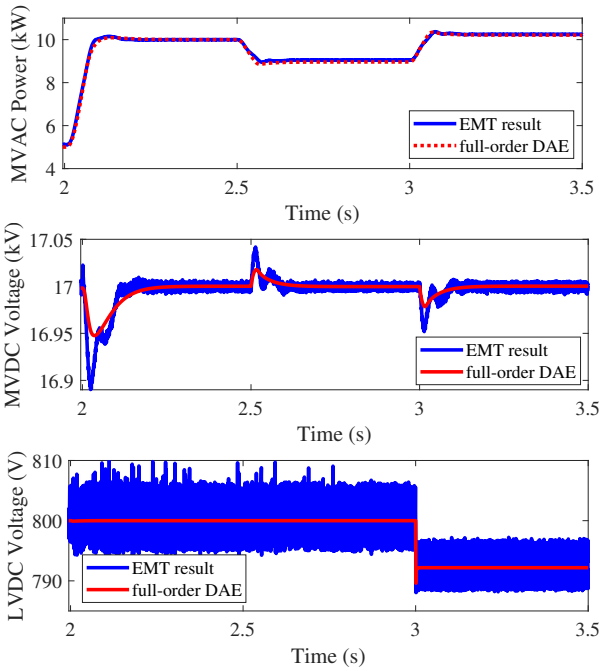

Fig. 5: Comparison of response from EMT model and full order DAE model of a 3 stage SST for setpoint changes.

parameters of the model for any given dynamic response under evaluation.

Let us consider the following sensitivities:

$$S_p = \left|\frac{\Delta P}{\Delta \Psi}\right| = \left|\frac{P_{\Psi,t} - P_{0,t}}{0.1\, P_{0,t}}\right|, \tag{17}$$

$$S_q = \left|\frac{\Delta Q}{\Delta \Psi}\right| = \left|\frac{Q_{\Psi,t} - Q_{0,t}}{0.1\, P_{0,t}}\right|, \tag{18}$$

Where Ψ represents the interested parameter, $P_{0,t}, Q_{0,t}$ are the grid power exchange from the ST at the time t using the original parameters, whereas $P_{\Psi,t}, Q_{\Psi,t}$ are the powers at the same time t as obtained by increasing parameter Ψ by 10% .

Based on the ST setup used in the hardware experiment, Fig. 7 shows which parameters the response is most sensitive at 1 ms, 10 ms and 100 ms respectively, following a grid voltage sag of 0.5 pu (graph on the left) or a grid frequency drop to 49.5 Hz (graph on the right). For the PI parameters, here we only show the sensitivity result of the proportional gain.

Figure 7 shows that, as expected, faster control dynamics can be neglected as the time scale increases. At 1 ms, the ST dynamics is mainly from the PSC current controller, not from the SSC. This is because the filter and dead-band of the SSC demand control do not initially allow the state of the SSC to vary. As the time scale increases, the effect of the current control dynamics weakens and that of the voltage controller dynamics increases as does the demand control. At 100 ms, fast ST dynamics are less relevant and the effect of the services on ST transient response becomes visible. On the other hand, the transients of the SSC and PSC are decoupled.

The response to the voltage sag is mainly from the PSC with DC voltage control and voltage support, whereas the response to the grid frequency drop is from the SSC with demand

control and SSC voltage control. Note that the demand control changes the ST power flow resulting in the PCC voltage variation, thus, activating the voltage support. From this parameter sensitivity analysis, the model can be simplified based on the time scale of research interest. These approximated models are presented in the remainder of this section.

A. Approximated Model based on Time Scales

If the time scale of interest is 10 ms, i.e., fast frequency response, the transients of the current controllers and DAB

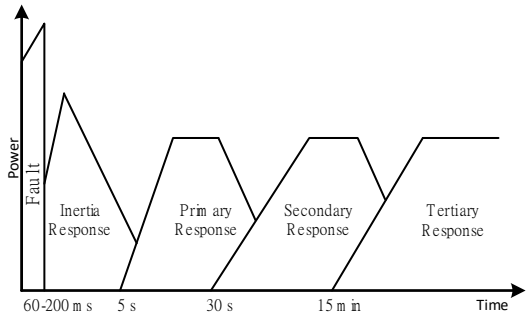

(a) Power system

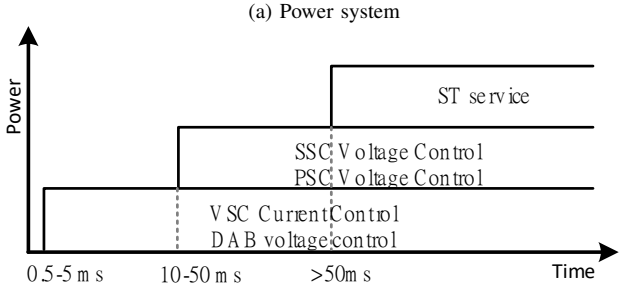

(b) Smart transformer

Fig. 6: Transient response time scales of interest.

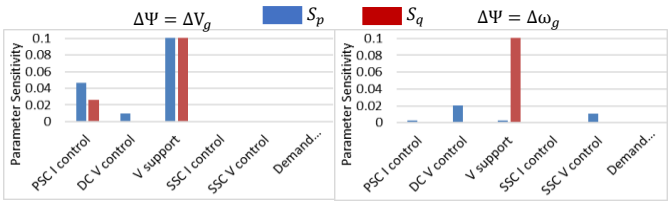

(a) Parameter sensitivity at 1 ms

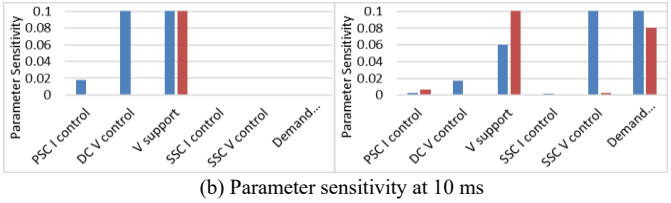

(b) Parameter sensitivity at 10 ms

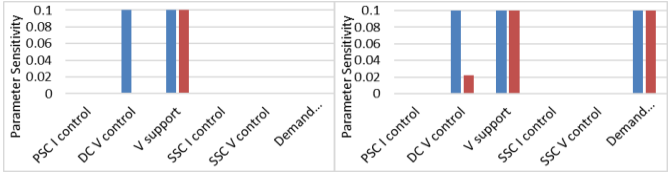

(c) Parameter sensitivity at 100 ms

Fig. 7: Smart transformer parameter sensitivity

voltage controller are negligible as well as line and filter transients. The relevant models at PSC stage (1)(2)(6), DAB stage (8)(9) and at SSC stage (13)(15) can be simplified as follows:

$$\begin{aligned} P_g &= V_g \cos(\delta_g - \delta_{pll}) I^*_{d,psc} + V_g \sin(\delta_g - \delta_{pll}) I^*_{q,psc}\,, \\ Q_g &= V_g \sin(\delta_g - \delta_{pll}) I^*_{d,psc} - V_g \cos(\delta_g - \delta_{pll}) I^*_{q,psc}\,, \\ V_{d,psc} &= V_g \cos(\delta_g - \delta_{pll}) - \omega_g L_g I^*_{q,psc}\,, \\ V_{q,psc} &= V_g \sin(\delta_g - \delta_{pll}) + \omega_g L_g I^*_{d,psc}\,, \end{aligned} \tag{19}$$

$$-C_{dcm} V_{dcm} \dot{V}_{dcm} = (V_{d,psc} I^*_{d,psc} + V_{q,psc} I^*_{q,psc}) + P_{psc}\,, \tag{20}$$

$$V_{dcl} = V^*_{dcl}\,, \tag{21}$$

$$\begin{aligned} C_{ssc} \dot{V}_{d,ssc} &= I^*_{d,psc} - I_{d,lvac} + \omega C_{ssc} V_{q,ssc}\,, \\ C_{ssc} \dot{V}_{q,ssc} &= I^*_{q,psc} - I_{q,lvac} - \omega C_{ssc} V_{d,ssc}\,. \end{aligned} \tag{22}$$

If the time scale of interest is 100 ms, i.e., primary response, all the converter related transients are negligible and only the transients of ST service need to be captured. Based on the above 10 ms model, PSC and SSC voltages are assumed to track their references instantaneously:

$$V_{dcm} = V^*_{dcm}\,, \tag{23}$$

and

$$V_{d,ssc} = V^*_{d,ssc};\ V_{q,ssc} = V^*_{q,ssc}\,. \tag{24}$$

The set of equations of the approximated ST models for the 10 ms and 100 ms time scales are summarized in Table III. The time step indicated in the last row of the table is set as 1/10 of the smallest time constant of the controller in the model.

TABLE III: Summary of the ST models.

ST Stage	Full model	10 ms model	100 ms model
PSC	(1)-(7)	(3)-(5),(7),(19),(20)	(5),(7),(19),(20),(23)
DAB	(8)-(11)	(8),(11),(21)	(8),(11)(21)
SSC	(12)-(16)	(12),(14),(16),(22)	(12),(16),(24)
Time step	0.1 ms	1 ms	10 ms

B. Approximated Model based on Research Focus

The ST only passes the active power while the reactive power is decoupled in each port as well as its voltage. It can be seen in Fig. 4 and Fig. 5 that the DC voltage has a transient response to the power variation but this transients barely affect the response of the PSC at the MVAC side. Due to this feature, according to the research focus, only the interested ST stage needs to be precisely modelled while other stags may be simplified or even neglected.

For example, in Fig. 7, when the grid voltage sags, the functional stage is the PSC while SSC barely has reactions. In this case, the model of the SSC could be neglected. However, when the grid frequency drops, the functional stage is the SSC, while PSC only needs to detect the frequency via PLL. In this case, the model of the PSC may be simplified.

Here we shall highlight the precondition of the model simplification in particular stage is that the operation of the

unconcerned stages are stable. Otherwise the voltage of the unstable converter collapses and its power oscillates, this oscillating power will go into the interested stage and affect its dynamic response, in this situation, a full model must be used.

IV. Use Cases

This section defines the use cases of the ST models proposed in this paper. These consider the following scenarios: faults, power exchange and provision of system services. A 3-stage ST model built in Matlab/Simulink is utilised to obtain simulation results. The complete set of parameters of the ST is given in Table IV, where a large grid impedance is selected here in order to purposely trigger the transient instability of the ST during the fault; a large filter of the PSC is then selected for a stable operation under the normal conditions; the parameters of the PI controller in the outer voltage and inner current are setup based on reference [24].

TABLE IV: ST parameters and settings.

Parameter	Value
V^*_{psc}	10 kV
V^*_{dcl}	800 V
Sn	50 MVA
$K_{pc,psc}/K_{ic,psc}$	2000 / 20000
$K_{p,pll}/K_{i,pll}$	0.022 / 0.39
$K/f_m/L_m$	20/10 kHz / 15 mH
L_{ssc}/r_{ssc}	6.9 mH / 0.012 Ω
$K_{pc,ssc}/K_{ic,ssc}$	69 / 553
K_v/K_{dab}	0.0000059 / 5
V^*_{dcm}	17 kV
V^*_{ssc}	330 V
$L_g/L_{psc}/r_{psc}$	0.5 H / 1 H / 0.1 Ω
$K_{p,dc}/K_{i,dc}$	0.001 / 0.0002
C_{dcm}/C_{dcl}	13.6 μF / 0.2 mF
$K_{p,dcl}/K_{i,dcl}$	0.41 / 0.15
C_{ssc}	0.2 mF
$K_{pv,ssc}/K_{iv,ssc}$	1 / 1100
$K_d/K_m/LP_f$	0.05 / 0.05 / 628

Initial	Value
P^*_{psc}/Q^*_{psc}	-4.1 MW / 0 MW
I_{lvdc}	1 A
I_{mvdc}	2 A
loading	26 Ω

A. Fault Response

According to grid codes, a fault should be cleared within 40 to 100 ms. The response of the converter to the fault is very fast, in the order of ms. The synchronization stability analysis of the converter consists in identifying whether the converter can ride through the fault. This section discusses the accuracy of the three ST models of Table III following a fault occurring in either the transmission or the distribution system.

1) Fault in the Transmission System: In this scenario, the fault occurs at the transmission side, i.e., the grid voltage sags from 1 pu to 0.34 pu at 2 s. Figure 8 shows the active power response of the ST at the MVAC side in the first 100 ms after the fault. The full model shows a peak power at the instant of the fault and an unstable response after, while the simplified models fail to capture such instability but represent a stable response. This is because although the PSC uses constant power control, ultimately it is a voltage source converter, whose terminal voltage cannot change instantaneously following the fault occurrence. This give raise to a high fault current and a peak power. In this case, neglecting the converter current controller dynamics results in an inaccurate transient behavior of the ST. Comparing with the 10 ms model, the 100 ms model only captures the PLL dynamics at the instant of the fault occurrence and, thus, reaches the steady-state faster than the 10 ms model.

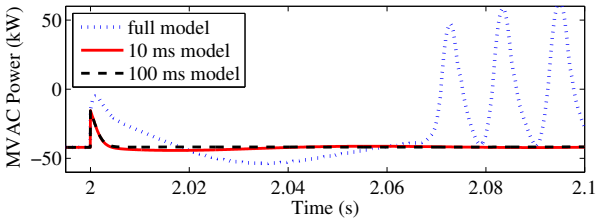

Fig. 8: Transmission system fault: time-scale model comparison.

The response of the ST with respect to the fault in the transmission system is mainly due to the PSC transients, thus, the DAB and SSC model can be simplified. Figure 9 shows the ST response using a detailed PSC model and simplified SSC and DAB models. Since the PSC model is not simplified, all models show the same response on the active power at the MVAC side and the voltage at the MVDC as shown in the first and second panels of Fig. 9. Neglecting the dynamic of the DAB voltage in the model "DAB 100 ms mode" worsens the accuracy at the LVDC side. The LVDC voltage, in fact, fails to capture the oscillations due to the instability of the PSC. The simplification of the SSC and DAB models make them unable to capture the interactions among the ST stages as shown in the lower panel of Fig. 9. These interactions, in fact, depend on the filter capacitance on the MVDC, LVDC and LVAC ports.

Since the instability is attributed to the PSC at the MVAC side, the DAB and SSC lose stability stage by stage in sequence as shown in Fig. 9. During this process, as long as the modulation does not hit the limitation, the downstream converter is in the control. Thus, the LVDC and LVAC voltage are still in a safe operation range even the MVAC and MVDC voltage collapsed. As a consequence, the transient power delivered through DAB, P_{dab}, barely has an effect on the PSC, that is the reason that "DAB 100 ms model", although loses the accuracy and shows a fixed voltage response at the LVAC and LVDC side, still can capture the response at the MVDC and MVAC side similar to the full model. In this situation, if the focus is solely on the transmission system over a small-time scale, the ST can be modelled by a detailed PSC with a constant P_{dab} to represent the total loading from the DAB. However, over a longer time, when the corresponding port voltage collapses, the power would change significantly, and then the full model must be used for a precise reflection of

ST dynamics.

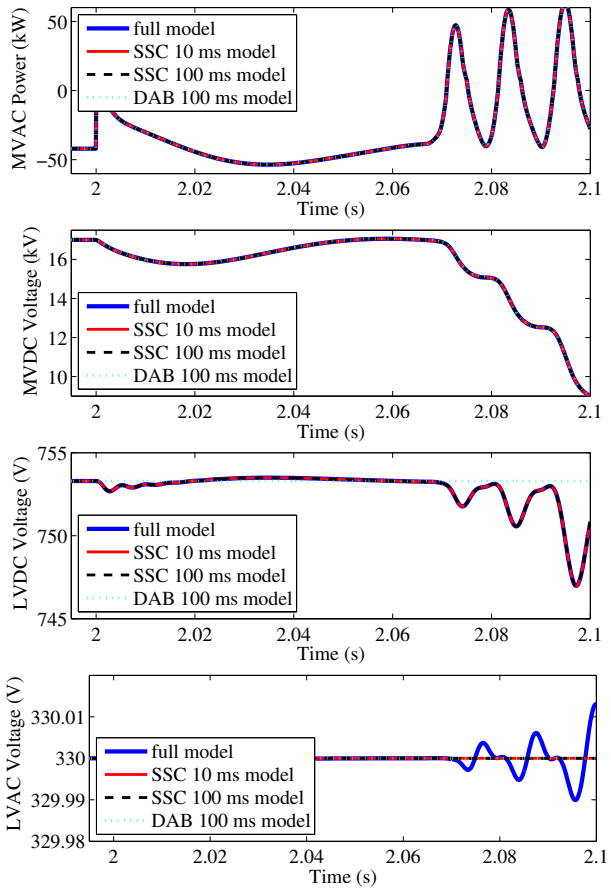

Fig. 9: Transmission system fault: stage model comparison.

2) Fault in the Distribution System: In this scenario, the fault occurs at the distribution system side. The loading impedance changes from 26 Ω to 1 Ω. The current limiter is set to be 30 A. Figure 10 shows the voltage response of the ST at the LVAC side and the active power at the MVAC side. Both the full-order model and the 100 ms model show the LVAC voltage sag following the fault occurrence. Neglecting the voltage controller dynamics leads to an inaccurate ST response, because the current limiter is also neglected. On the other hand, the high power at the instant of the fault occurrence is due to the constant SSC voltage. If the LVAC voltage decreases, the total ST power consumption also decreases.

The stage of the ST that is most sensitive to a fault in the distribution system side is the SSC. Hence the models of the other stages can be simplified. Figure 11 shows the response of the ST with full-order SSC model and simplified models for the PSC and DAB. The results show that as long as the SSC part is accurately modeled, the LVAC voltage dynamics can be precisely captured regardless of the modeling of the other stages. Thus, if the research interest is solely on the distribution system, the ST can be modelled by a detailed SSC. However, an accurate DAB model can capture the LVDC voltage dynamics due to the transient power exchange amongst DAB and SSC.

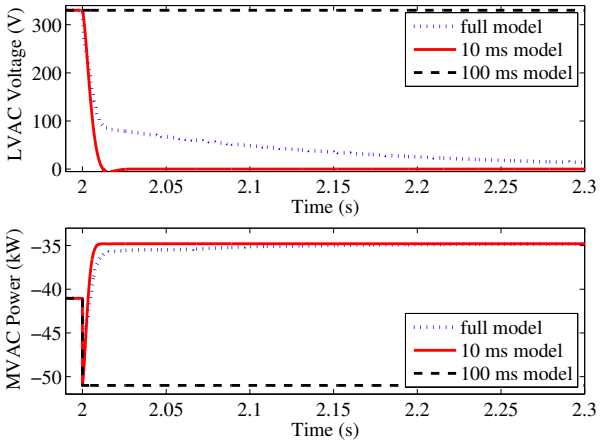

Fig. 10: Distribution system fault: time-scale model comparison.

B. DC Power Exchange

The ability to regulate the power exchange among the ST subsystems is a relevant feature of the ST. A proper ST model has to precisely capture its dynamic behavior during these power exchanges. Since the power exchange initiated at the AC ports is discussed in Section IV-C, this section focuses on the DC power exchange.

Figure 12 shows the ST transient response following a step increase of the LVDC loading from 1 A to 4 A at 2 s and a step decrease of the MVDC loading current from 2 A to 1.8 A. Due to the fast reaction of the DAB voltage controller, the DC power exchange only introduces a small disturbance and these transients damps quickly within 50 ms. As long as the DAB voltage controller is precisely modeled, the ST transients can be well captured regardless the modeling of the SSC and PSC stages.

C. ST Services

The conventional primary frequency and voltage control of synchronous machines is in the time scale of seconds. Correspondingly, the model of the ST for the system services only needs to retain the dynamics in the time scale of second. This subsection presents the ST model aimed at retaining the dynamics of the primary frequency and voltage support, respectively.

1) Frequency Support: In this scenario, a grid frequency drop from 50 Hz to 49 Hz occurs at 2 s with 1 Hz/s ramp. From the grid point of view, only the active power at the at the MVAC bus of the ST is of interest. Figure 13 shows that the active power responses for all ST models are identical. This is because the power change is smooth and, thus, the dynamics of the ST current and voltage controllers are immaterial and can be neglected. Note that the power does not change instantaneously following the frequency variation because of the dead-band and low-pass filter in the ST demand control.

2) Voltage Support: In this scenario, a grid voltage drop from 1 pu to 0.95 pu occurs at 2 s. From the grid point of view, only the reactive power at the MVAC bus of the ST is of interest. Figure 14 shows that the reactive power response

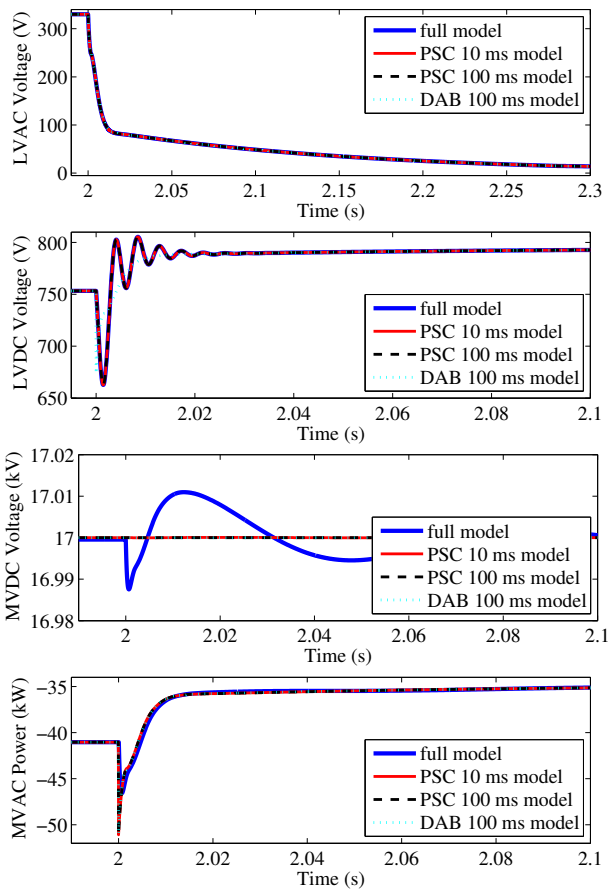

Fig. 11: Distribution system fault: stage model comparison.

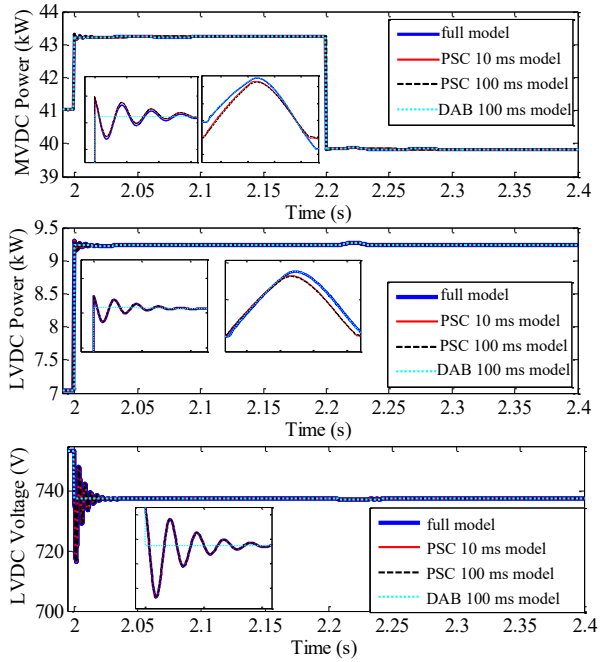

Fig. 12: DC power exchange: time-scale and stage model comparison.

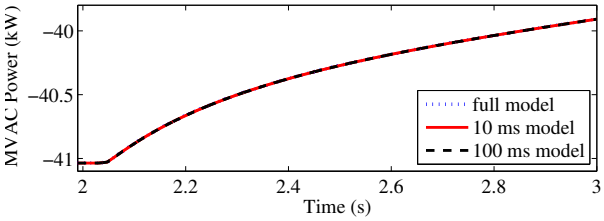

Fig. 13: ST frequency support: time-scale model comparison.

of different ST model is significantly different only in the first 100 ms after the voltage drop. The transient response of these models in the first 100 ms is similar to that of a fault on the transmission system side, where the PSC must be precisely modeled. However, in this case, the time scale of interest is of the order of seconds and, thus, the differences in the first 100 ms is negligible. This makes the 100 ms ST model adequate for this use case.

V. Case Study

The main purpose of the ST models proposed in this paper is for the analysis of power system transients. With this aim, this case study considers different ST models in a modified New England 39-bus system, where 40% of the load is assumed to be connected to the grid through 4 STs at buses 4, 8, 20 and 39, as shown in Fig. 15. The New England 39-bus system includes Automatic Voltage Regulations (AVRs) and Turbine Governor (TG) for each synchronous machine [15]. The loads are modeled as voltage dependent with its exponent in the range of 0.1 to 1.5.

In accordance with the use case of the model defined in Section IV, the case study considers three scenarios: a fault, a DC generation increase, and a generator outage. All simulations in this section are solved with DOME, a Python-based power system software tool [25]. Simulations are carried out with a Dell Inspiron with 4 Intel Core i5 2.5 GHz. The computation time of the full, 10-ms and 100-ms models for the fault scenario are 197.8 s, 23.65 s and 3.131 s, respectively.

A. Scenario 1: Fault

This scenario considers a fault on line 1-2 occurring at 1 s and cleared in 40 ms. Figure 16 shows the response of the power of ST4 and the system response, namely the grid frequency and the voltage at bus 39. At the instants of the fault occurrence and clearance, the full model shows a transient peak in the power. These peaks corresponds to voltage transients at ST PCC buses. However, this phenomenon can only be captured via the full model. The simplified models cannot reproduce these transients as they do not retain the dynamics of converter currents. On the other hand, the response of the system frequency is similar for the three models as it is mainly driven by the synchronous machines and their controllers.

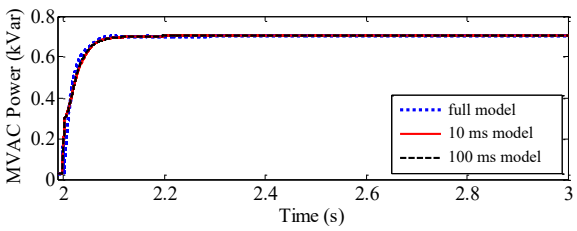

Fig. 14: ST voltage support: time-scale model comparison.

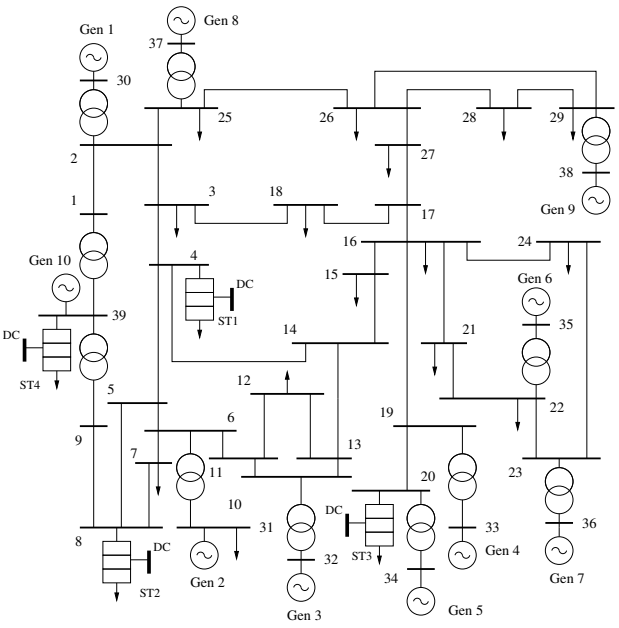

Fig. 15: Modified New England 39-bus system.

B. Scenario 2: ST DC power generation

This scenario considers the DC current of the STs following a DC power generation step increase from 0 to 1 pu at 1 s. Figure 17 shows the ST4 power response, the grid frequency and the voltages bus 39. As shown in the use case of DC power exchange in Section IV-B, the transients of the DC power is very small and damps quickly. The power decrease following the current step change is due to the ST demand control in response to the frequency increase. The system frequency and voltage response are similar and independent from the ST model.

C. Scenario 3: Generator Outage

This scenario considers the outage of the generator at bus 34 at 1 s. Figure 18 shows the grid frequency and the voltage at Bus 39. Similarly to the use case discussed in Section IV-C, all ST models are equivalent in the time scale of frequency and voltage stability analysis. This means that the simplest ST model can be utilized without loss of information.

VI. Conclusion

This paper proposes a 3×3 set of ST models according to the time scales, and classifies these models based on a set of use cases. The following relevant conclusions are supported by simulation results.

- For the analysis of the transients following a fault occurring in the transmission system, the PSC of the ST must be precisely modelled. A simplification of the PSC current dynamics erroneously increases the ST operational region and fails to capture the voltage transients. On the other hand, the DAB and SSC model can be simplified or even neglected, depending on the fault duration without loss of accuracy, if the LVDC and LVAC voltage is not of interest.

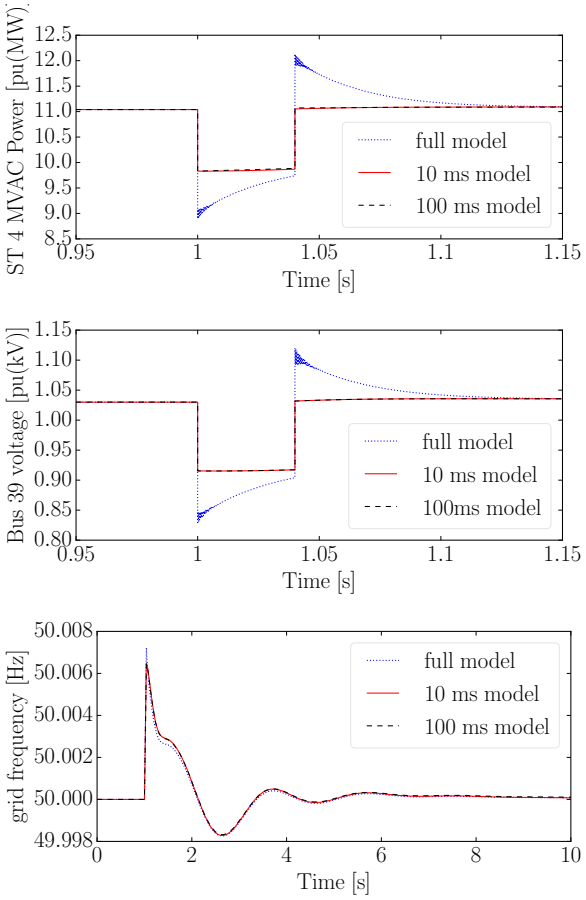

Fig. 16: New England 39-bus system, Scenario 1: fault.

- For the analysis of the transients following a fault occurring in the distribution system, the SSC of the ST must be precisely modelled. A simplification of the SSC current dynamics disables the current limitation thus fails to capture the voltage transients. On the other hand, the PSC and DAB model can be neglected without loss of accuracy, if the LVDC, MVDC and MVAC voltage are not of interest.
- The simplest ST model is adequate for frequency and voltage stability analysis.

References

[1] F. Milano, F. Dörfler, G. Hug, D. J. Hill, and G. Verbič, "Foundations and challenges of low-inertia systems (invited paper)," in *2018 Power Systems Computation Conference (PSCC)*, 2018, pp. 1–25.

[2] X. She, A. Q. Huang, and R. Burgos, "Review of solid-state transformer technologies and their application in power distribution systems," *IEEE Journal of Emerging and Selected Topics in Power Electronics*, vol. 1, no. 3, pp. 186–198, 2013.

[3] M. Liserre, G. Buticchi, M. Andresen, G. De Carne, L. F. Costa, and Z. Zou, "The smart transformer: Impact on the electric grid and technology challenges," *IEEE Industrial Electronics Magazine*, vol. 10, no. 2, pp. 46–58, 2016.

[4] A. Q. Huang, M. L. Crow, G. T. Heydt, J. P. Zheng, and S. J. Dale, "The future renewable electric energy delivery and management (freedm) system: The energy internet," *Proceedings of the IEEE*, vol. 99, no. 1, pp. 133–148, 2011.

[5] X. Yu, X. She, X. Zhou, and A. Q. Huang, "Power management for dc microgrid enabled by solid-state transformer," *IEEE Transactions on Smart Grid*, vol. 5, no. 2, pp. 954–965, 2014.

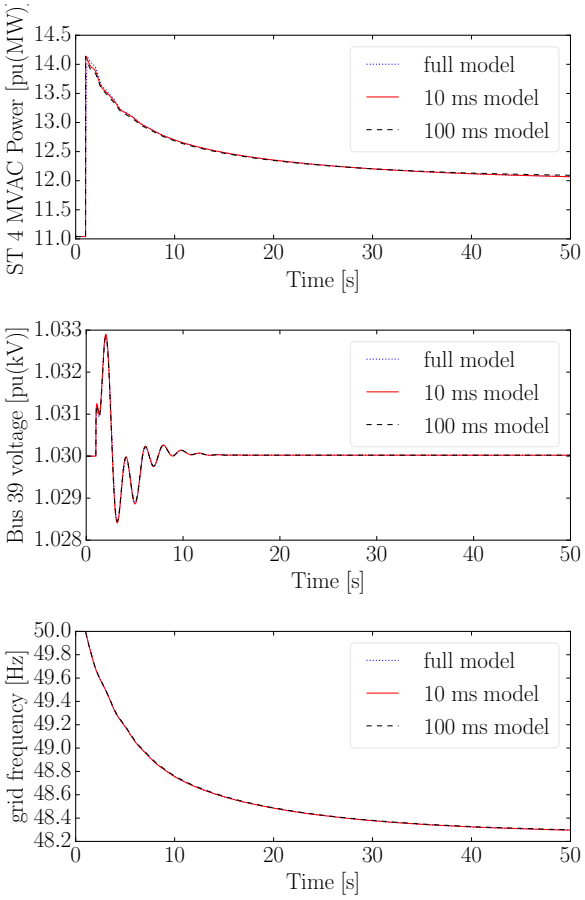

Fig. 17: New England 39-bus system, Scenario 2: DC generation.

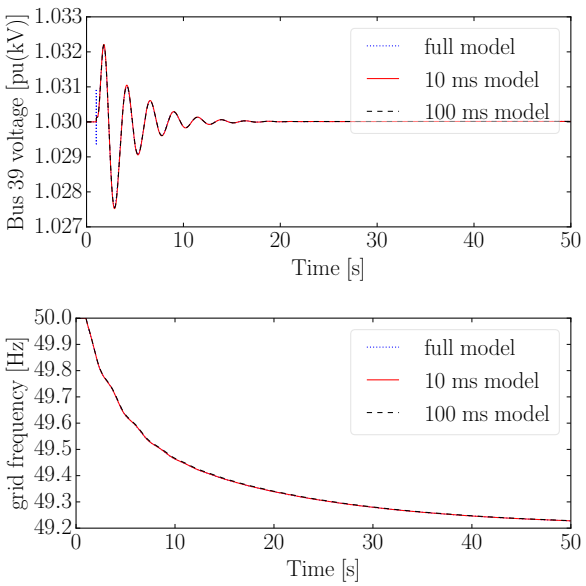

Fig. 18: New England 39-bus system, Scenario 3: system contingency.

[6] X. Gao, F. Sossan, K. Christakou, M. Paolone, and M. Liserre, "Concurrent voltage control and dispatch of active distribution networks by means of smart transformer and storage," *IEEE Transactions on Industrial Electronics*, vol. 65, no. 8, pp. 6657–6666, 2018.

[7] Z. Zou, G. De Carne, G. Buticchi, and M. Liserre, "Smart transformer-fed variable frequency distribution grid," *IEEE Transactions on Industrial Electronics*, vol. 65, no. 1, pp. 749–759, 2018.

[8] J. Chen, M. Liu, G. De Carne, R. Zhu, M. Liserre, F. Milano, and T. O'Donnell, "Impact of smart transformer voltage and frequency support in a high renewable penetration system," *Electric Power Systems Research*, vol. 190, p. 106836, 2021. [Online]. Available: http://www.sciencedirect.com/science/article/pii/S0378779620306362

[9] G. De Carne, G. Buticchi, M. Liserre, and C. Vournas, "Load control using sensitivity identification by means of smart transformer," *IEEE Transactions on Smart Grid*, vol. 9, no. 4, pp. 2606–2615, 2018.

[10] G. De Carne, M. Liserre, and C. Vournas, "On-line load sensitivity identification in lv distribution grids," *IEEE Transactions on Power Systems*, vol. 32, no. 2, pp. 1570–1571, 2017.

[11] J. Chen, T. Yang, C. O'Loughlin, and T. O'Donnell, "Neutral current minimization control for solid state transformers under unbalanced loads in distribution systems," *IEEE Transactions on Industrial Electronics*, vol. 66, no. 10, pp. 8253–8262, 2019.

[12] J. Chen, R. Zhu, I. Ibrahim, T. O'Donnell, and M. Liserre, "Neutral current optimization control for smart transformer-fed distribution system under unbalanced loads," *IEEE Journal of Emerging and Selected Topics in Power Electronics*, vol. 9, no. 2, pp. 1696–1707, 2021.

[13] D. Shah and M. L. Crow, "Online volt-var control for distribution systems with solid-state transformers," *IEEE Transactions on Power Delivery*, vol. 31, no. 1, pp. 343–350, 2016.

[14] G. De Carne, M. Langwasser, M. Ndreko, R. Bachmann, R. W. De Doncker, R. Dimitrovski, B. J. Mortimer, A. Neufeld, F. Rojas, and M. Liserre, "Which deepness class is suited for modeling power electronics?: A guide for choosing the right model for grid-integration studies," *IEEE Industrial Electronics Magazine*, vol. 13, no. 2, pp. 41–55, 2019.

[15] F. Milano, *Power System Modelling and Scripting*. London: Springer, 2010.

[16] J. Chen, R. Li, A. Soroudi, A. Keane, D. Flynn, and T. O'Donnell, "Smart transformer modelling in optimal power flow analysis," in *IECON 2019 - 45th Annual Conference of the IEEE Industrial Electronics Society*, vol. 1, 2019, pp. 6707–6712.

[17] J. Miao, N. Zhang, C. Kang, J. Wang, Y. Wang, and Q. Xia, "Steady-state power flow model of energy router embedded ac network and its application in optimizing power system operation," *IEEE Transactions on Smart Grid*, vol. 9, no. 5, pp. 4828–4837, 2018.

[18] T. Zhao, J. Zeng, S. Bhattacharya, M. E. Baran, and A. Q. Huang, "An average model of solid state transformer for dynamic system simulation," in *2009 IEEE Power Energy Society General Meeting*, 2009, pp. 1–8.

[19] A. A. Milani, M. T. A. Khan, A. Chakrabortty, and I. Husain, "Equilibrium point analysis and power sharing methods for distribution systems driven by solid-state transformers," *IEEE Transactions on Power Systems*, vol. 33, no. 2, pp. 1473–1483, 2018.

[20] Y. Tu, J. Chen, H. Liu, and T. O'Donnell, "Smart transformer modelling and hardware in-the-loop validation," in *2019 IEEE 10th International Symposium on Power Electronics for Distributed Generation Systems (PEDG)*, 2019, pp. 1019–1025.

[21] M. Lee, J. Kim, and J. Lai, "Small-signal modeling of three-level boost rectifier and system design for medium-voltage solid-state transformer," in *2019 10th International Conference on Power Electronics and ECCE Asia (ICPE 2019 - ECCE Asia)*, 2019, pp. 1–7.

[22] Q. Ye, R. Mo, and H. Li, "Impedance modeling and dc bus voltage stability assessment of a solid-state-transformer-enabled hybrid ac–dc grid considering bidirectional power flow," *IEEE Transactions on Industrial Electronics*, vol. 67, no. 8, pp. 6531–6540, 2020.

[23] M. T. A. Khan, A. A. Milani, A. Chakrabortty, and I. Husain, "Dynamic modeling and feasibility analysis of a solid-state transformer-based power distribution system," *IEEE Transactions on Industry Applications*, vol. 54, no. 1, pp. 551–562, 2018.

[24] A. Yazdani and R. Iravani, *Voltage-Sourced Converters in Power Systems : Modeling, Control, and Applications*. New Jersy: John Wiley & Sons, Inc., 2014.

[25] F. Milano, "A Python-based software tool for power system analysis," in *IEEE PES General Meeting*, 2013, pp. 1–5.